Dalton Transactions

PAPER

Cite this: *Dalton Trans.*, 2015, **44**, 14666

Systematic design of secondary building units by an efficient cation-directing strategy under regular vibrations of ionic liquids†

Bing An,‡[a] Jun-Li Wang,‡[a] Yan Bai*[a,b] and Dong-Bin Dang*[a]

Received 28th April 2015,
Accepted 10th July 2015

DOI: 10.1039/c5dt01595b

www.rsc.org/dalton

A cobalt-1,4-naphthalenedicarboxylic acid system in a systematic series of ionic liquids with different alkyl chain lengths of imidazolium cations governed the construction of four MOFs with regular changes of secondary building units (SBUs).

Introduction

A strategy for stitching metal ions and organic carboxylate linkers into extended networks has advanced to a point that allows the designed metal–organic frameworks' (MOFs') structure and functionality to be varied systematically.[1] Apparently, a system of organization may be mooted for chemists to facilitate the expansion of the MOF family. The modular concept allows for a rational design of MOFs in which a metal oxide cluster named the secondary building unit (SBU) is used as a connecting node and organic spacers of different lengths are used to link the nodes into a three-dimensional network with predefined topology.[2] SBUs where each metal ion is locked into position by the carboxylates have the relevant attributes necessary to assemble the skeleton of the desired structure.[3] However, systematic modulation of SBUs with similar properties, such as size and shape, is a big challenge. It is difficult to change the structures systematically with the same metal–ligand source at the same temperature by the traditional hydro/solvo-thermal method, because the structural modification leads to unpredictable results and is hard to systematically control.

Ionic liquids (ILs) made from cations and anions are fluid at near-ambient temperature (less than ~100 °C) and have virtually no vapor pressure.[4] Since the synthesis of the first 3D MOF $[Cu_3(tpt)_4](BF_4)_3\cdot(TPT)_{2/3}\cdot 5H_2O$ (TPT = 2,4,6-tris(4-pyridyl)-1,3,5-triazine) was reported by Kim *et al.* in 2004 using an IL,[5] ionothermal synthesis has emerged as a promising means to open up new research directions. Pioneering studies have proven that the cation and the anion can individually or cooperatively influence the resulting MOF structures.[6] Lightfoot and colleagues discovered that the specific solvent properties of imidazolium ILs can control and stabilize a particular oxidation state of the metallic species.[7] Since the size of ILs can be tailored, it follows naturally to systematically probe the structure-directing agents (SDAs) using ILs that vary in structure. Thus, ILs based on the 1-alkyl-3-methylimidazolium cation (abbreviated $[C_nMIm]^+$, where n is the number of carbon atoms in a linear alkyl chain) are good candidates.

The appropriate nature of organic ligands is undoubtedly a key element in exploring ILs as SDAs to control the microarchitecture of frameworks. Up to now, only the Ni/Zn-1,3,5-benzenetricarboxylate acid (BTC) system with variation of the alkyl chain length has been reported.[8] BTC has various coordination modes allowing it to assemble desirable frameworks. For that reason, it makes it difficult to investigate a regular change in the structures. Our current interest is in the introduction of 1,4-naphthalenedicarboxylic acid (1,4-H_2ndc) as an organic linker due to its favourable rigidity and suitable spacer length.[9] Herein, we report a system in which the nature of the IL cations governs general structural features by increasing the alkyl chain length from two to five carbon atoms. The system we explored was the $Co(NO_3)_2$-1,4-H_2ndc system with [RMIm]-Br (R = ethyl (EMIm), propyl (PMIm), butyl (BMIm) and amyl (AMIm)). Four novel cobalt frameworks [EMIm][Co(1,4-ndc)Br] (**1**), $[PMIm]_2[Co_7(1,4\text{-ndc})_6(OH)_4]$ (**2**), $[BMIm]_2[Co_6(1,4\text{-ndc})_6(OH)_2]$ (**3**) and $[AMIm]_4[Co_4Na_5(1,4\text{-ndc})_8Br]$ (**4**) were obtained. We attempted to determine whether it is possible to modulate the size and shape of high nuclear Co-clusters and then influence the magnetic properties by tuning the SBUs.

[a]*Henan Key Laboratory of Polyoxometalate Chemistry, Institute of Molecular and Crystal Engineering, College of Chemistry and Chemical Engineering, Henan University, Kaifeng 475004, P. R. China. E-mail: baiyan@henu.edu.cn, dangdb@henu.edu.cn; Fax: (+86)-371-23881589; Tel: (+86)-371-23881589*

[b]*State Key Laboratory of Coordination Chemistry, Nanjing University, Nanjing 210093, P. R. China*

†Electronic supplementary information (ESI) available: Experimental details; crystal data, additional figures, TG curves, XRPD and magnetic properties. CCDC 1034908–1034911. For ESI and crystallographic data in CIF or other electronic format see DOI: 10.1039/c5dt01595b

‡These authors contributed equally.

Experimental section

Materials and methods

All reagents were used as purchased without further purification. ILs: [EMIm]Br, 1-ethyl-3-methylimidazolium bromide; [PMIm]Br, 1-propyl-3-methylimidazolium bromide; [BMIm]Br, 1-butyl-3-methylimidazolium bromide; [AMIm]Br, 1-amyl-3-methylimidazolium bromide were synthesized by a previously reported procedure.[10] Elemental analyses (C, H and N) were performed with a Perkin-Elmer 2400-II CHN analyzer. IR spectra were recorded on a Nicolet 360 FT-IR spectrometer using KBr pellets in the range of 4000–400 cm^{-1}. The thermogravimetric analyses were carried out under a nitrogen atmosphere on a Perkin-Elmer-7 thermal analyzer at a heating rate of 10 °C min^{-1} from 25 to 850 °C. The crystalline samples of **1–4** were identified at room temperature by powder X-ray diffraction (PXRD) using a Philips X'Pert Pro Super diffractometer with graphite monochromatized Cu Kα radiation (λ = 1.54178 Å). Magnetic susceptibility data on crushed single crystals were collected over the temperature range 2–300.0 K using a Quantum Design MPMS-5S super-conducting quantum interference device (SQUID) magnetometer.

Syntheses of 1–4

[EMIm][Co(1,4-ndc)Br] (1). A mixture of 1,4-H_2ndc (1 mmol, 0.210 g), NaOH (2 mmol, 0.080 g), $Co(NO_3)_2{\cdot}6H_2O$ (3 mmol, 0.873 g) and [EMIm]Br (2 g) was transferred to a 25 mL Teflon-lined steel autoclave and kept at 160 °C for 5 days under autogenous pressure. After naturally cooling down to room temperature, dark blue crystals of **1** were obtained. Anal. Calcd (found %) for $C_{18}H_{17}BrCoN_2O_4$: C 46.66 (46.52), H 3.70 (3.61), N 6.05 (5.96). IR (cm^{-1}, KBr pellet): 3437(w), 3161(w), 3101(w), 2984(w), 2940(w), 1620(s), 1573(m), 1511(w), 1466(m), 1421(s), 1371(s), 1312(w), 1271(w), 1213(w), 1169(m), 1032(w), 971(w), 857(w), 823(m), 793(w), 764(m), 744(w), 619(w), 568(m), 452(w), 417(w).

$[PMIm]_2[Co_7(1,4\text{-ndc})_6(OH)_4]$ (2). The blue block crystals of **2** were prepared in the same way as for **1**, except that [PMIm]Br (2 g) was used instead of [EMIm]Br. Anal. Calcd (found %) for $C_{86}H_{66}Co_7N_4O_{28}$: C 51.22 (51.35), H 3.30 (3.42), N 2.78 (2.70). IR (cm^{-1}, KBr pellet): 3412(w), 3142(w), 3068(w), 2970(w), 2933(w), 1594(s), 1567(s), 1512(m), 1462(m), 1417(s), 1366(s), 1312(w), 1262(w), 1214(w), 1173(w), 1036(w), 866(w), 824(w), 791(w), 767(m), 664(w), 623(w), 582(w), 556(w), 496(w), 455(w).

$[BMIm]_2[Co_6(1,4\text{-ndc})_6(OH)_2]$ (3). The blue block crystals of **3** were prepared in the same way as for **1**, except that [BMIm]Br (2 g) was used instead of [EMIm]Br. Anal. Calcd (found %) for $C_{80}H_{51}Co_6N_2O_{26}$: C 53.07 (52.89), H 2.84 (2.76), N 1.55 (1.47). IR (cm^{-1}, KBr pellet): 3435(w), 3143(w), 3067(w), 2959(w), 2930(w), 1619(s), 1553(s), 1513(w), 1464(m), 1413(s), 1369(s), 1311(w), 1264(w), 1212(w), 1165(w), 1115(w), 1032(w), 852(w), 834(w), 804(w), 787(w), 748(w), 665(w), 620(w), 581(w), 559(w), 453(w).

$[AMIm]_4[Co_4Na_5(1,4\text{-ndc})_8Br]$ (4). The dark blue block crystals of **4** were prepared in the same way as for **1**, except that [AMIm]Br (2 g) was used instead of [EMIm]Br. Anal. Calcd (found %) for $C_{132}H_{116}BrCo_4N_8Na_5O_{32}$: C 57.51 (57.63), H 4.24 (4.37), N 4.07 (4.15). IR (cm^{-1}, KBr pellet): 3437(w), 3146(w), 3079(w), 2959(w), 2932(w), 1599(s), 1572(s), 1511(w), 1459(m), 1414(s), 1353(s), 1262(w), 1209(w), 1166(w), 1119(w), 1032(w), 977(w), 869(w), 825(w), 804(w), 789(w), 765(w), 669(w), 573(w), 503(w), 447(w).

X-ray crystal structure determination

X-ray single crystal diffraction data for **1–4** were collected on a Bruker Apex-II CCD detector using graphite monochromatized Mo-Kα radiation (λ = 0.71073 Å) at room temperature. Routine Lorentz and polarization corrections were applied. The structures were solved by the direct method of SHELXS-97 and refined by the full-matrix least-squares method using the SHELXL-97 program package.[11] All of the non-hydrogen atoms were refined with anisotropic thermal displacement coefficients. Hydrogen atoms were assigned to calculated positions using a riding model with appropriately fixed isotropic thermal parameters.

Polymer **1** crystallizes in the monoclinic space group $P2_1/n$. The $[EMIm]^+$ cation was refined as disordered with the site occupancy factor (s.o.f.) of 0.5 except C(14′), C(14B) and C(15) with the s.o.f. of 0.25. Polymer **2** crystallizes in the orthorhombic *Pbca* space group. The s.o.f. of C(41), C(42), C(43) and O(4) atoms is refined as 0.5. Polymer **3** crystallizes in the monoclinic $C2/c$ space group. All the carbon atoms of the three 1,4-ndc^{2-} ligands are rotationally disordered over two orientations in the refined ratio 0.5 : 0.5 except C(1)–C(3), C(6), C(13)–C(15), C(18), C(25)–C(27) and C(30). The $[BMIm]^+$ cation was refined as disordered with the s.o.f. of 0.5 for all atoms. Polymer **4** crystallizes in the tetragonal space group $P4/n$. The carbon atoms C(30)–C(33) from the $[AMIm]^+$ cation are disordered over three positions in the refined ratio 0.33 : 0.33 : 0.33. The detailed crystallographic data and structure refinement parameters are summarized in Table S1.† Selected bond distances, bond angles and hydrogen bonding interactions are listed in Tables S2–S9.†

Results and discussion

Crystal structures of 1–4

Polymer **1** was synthesized from [EMIm]Br and is isostructural to the reported cadmium analogue [EMIm][CdBr(1,4-ndc)].[12] The whole framework is described as a two-dimensional (4,4)-connected anionic net constructed of paddle wheel-like $[Co_2(COO)_4]$ SBUs with 3.03 Å for the Co···Co distance and tetradentate μ_4–(μ_2–η1:η1)–(μ_2–η1:η1) bridged 1,4-ndc^{2-} ligands (Fig. S2†). Each rectangular void encapsulates $[EMIm]^+$ to compensate for the negative-charge of the framework.

When the length of the alkyl chain was increased, a 3D anionic framework **2** based on a heptanuclear cobalt cluster was formed. The asymmetric unit has four crystallographically independent cobalt(II) centers with Co(3) occupying the inversion center, three 1,4-ndc^{2-} ligands, two OH^- anions and one $[PMIm]^+$ cation (Fig. S3†). Co(1) and Co(4) are tetrahedrally co-

ordinated, and the Co(2) and Co(3) centers are in octahedra. The 1,4-ndc^{2-} ligand adopts a tridentate connectivity mode, μ_3–η1–(μ_2–η1:η1). Besides this, two μ_3-OH groups also participate in the coordination. These linkers connect seven cobalt atoms to form a hexapetalous flower-like heptanuclear cobalt SBU [$Co_7(\mu_3\text{-}O)_4(OCO)_{10}$]. Co(1), Co(2), Co(4) and their centrosymmetric equivalents are on the rim as petals, while the sole Co(3) hidden in the petals occupies the center. The Co···Co separations are 3.21 Å for Co1···Co2, 3.65 Å for Co1···Co3, 3.93 Å for Co1···Co4, 3.03 Å for Co2···Co3, 3.40 Å for Co2···Co4 and 3.53 Å for Co3···Co4. Such a shaped cluster comprising four $Co^{II}O_4$ tetrahedra *via* the vertex-sharing fashion connected to three edge-sharing $Co^{II}O_6$ octahedra, is drastically different from those found in the mixed-valent SBUs containing seven CoO_6 octahedra, such as [$Co^{II}_4Co^{III}_3$], [$Co^{II}_3Co^{III}_4$] and [$Co^{II}_6Co^{III}$].[13] Each heptanuclear SBU is linked to eight SBUs through twelve 1,4-ndc^{2-} ligands as four "double-bridges" along the *ab* plane with the distance of 12.59 Å and four "single-bridges" along the *bc* plane with a distance of 15.66 Å. Consequently, such a connection mode of SBUs extends to form a three-dimensional framework containing over two mutually perpendicular 2D layers. This results in an open porous channel (A) and a blocked narrow window (B) with [PMIm]$^+$ stacked (Fig. 1). Topologically, the overall 3D framework can be simplified as an eight-connected net with a ($4^{22}\cdot6^6$) short Schläfli symbol (Fig. S5†).

When the reaction was carried out in [BMIm]Br, the overall structure of **3** builds from chair conformational [$Co_6(\mu_3\text{-}O)_2(OCO)_{12}$] SBUs where Co(1) and Co(2) atoms adopt a distorted octahedral coordination geometry and Co(3) is tetrahedrally coordinated. The three crystallographically independent 1,4-ndc^{2-} anions exhibit three unprecedented types of bridging modes, μ_4–(μ_2–η1:η1)–(μ_2–η1:η1), μ_3–(η1:η1)–(μ_2–η1:η1) and μ_4–(μ_2–η2:η1)–(μ_2–η1:η1), all in one structure (Fig. 2). A centrosymmetric hexanuclear cobalt cluster [$Co_6(\mu_3\text{-}O)_2(OCO)_{12}$] containing two symmetry-related trinuclear units linked by a pair of μ_2–η2:η1 carboxylates adopts the unusual chair conformation with an inversion centre located mid-way along the Co(3)···Co(3D) vector. Co(1), Co(2) and Co(3) share one μ_3-OH bridge to form a triangular unit with the Co···Co separations of 3.25 Å–3.36 Å and the Co–μ_3-OH–Co angles of 57.81°–61.14°. At the same time, different Co(II) centers are linked by the Co–O–C–O–Co linkages as well. Although some hexanuclear cobalt complexes [$Co_6(OH)_2(PhCOO)_{10}(PhCOOH)_4$]·3$PhCH_3$, [$Co_3(C_6H(COO)_5)$-$(OH)(H_2O)_3$] and [$Co_6(OH)_2(L)_{10}$] have been reported,[14] the chair conformational hexanuclear SBU with two $Co(3)O_4$ tetrahedra *via* the vertices-sharing jointed four CoO_6 octahedra has never been found in cobalt frameworks. Furthermore, different from two kinds of modes, μ_2–η1:η1 and μ_3–η2:η1, in over three [Co_6] structures in the literature, the carboxylate groups in **3** exhibit more abundant coordination patterns including μ_2–η1:η1, μ_2–η2:η1 and η1:η1. The 3D structure of polymer **3** is similar to **2**. Each SBU connects with the surrounding eight SBUs through four μ_4–(μ_2–η1:η1)–(μ_2–η1:η1) "single-bridges" with a separation of 14.79 Å and four μ_3–(η1:η1)–(μ_2–η1:η1) and μ_4–(μ_2–η2:η1)–(μ_2–η1:η1) "double-bridges" with a separation of 13.02 Å in an SBU-1,4-ndc^{2-}-SBU fashion to generate a 3D ($4^{24}\cdot6^4$) framework (Fig. S8†).

Polymer **4**, synthesised from [AMIm]Br, contains two Na ions, one Co(II) ion, two 1,4-ndc^{2-} ligands, one Br^- anion and one [AMIm]$^+$ cation in the asymmetric unit (Fig. S9†). The 1,4-

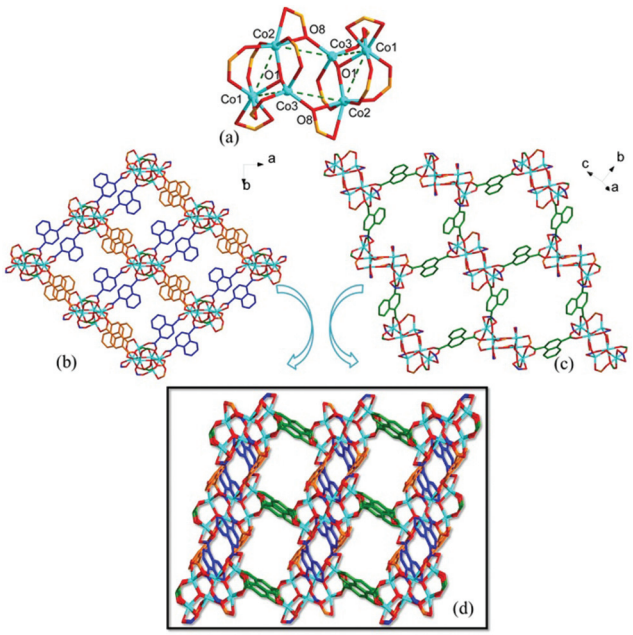

Fig. 2 (a) A hexanuclear SBU in the chair conformation. View of the two types of 2D layers constructed from the double-bridges (b) and single-bridge (c) in **3**. The green "single-bridge", and blue and orange "double-bridges" are μ_4–(μ_2–η1:η1)–(μ_2–η1:η1), μ_3–(η1:η1)–(μ_2–η1:η1) and μ_4–(μ_2–η2:η1)–(μ_2–η1:η1) 1,4-ndc^{2-} ligands, respectively. (d) The 3D framework of **3** with two kinds of 1D channel along the *b* axis; the [BMIm]$^+$ cations are omitted for clarity.

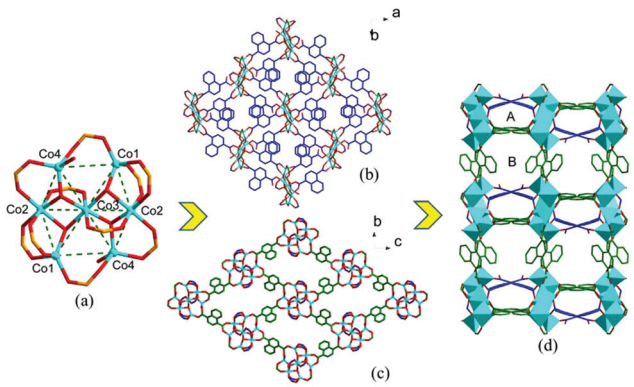

Fig. 1 View of the two types of 2D layers of **2**. (a) Illustration of the heptanuclear SBU. (b) The blue "double-bridges" are μ_4–(μ_2–η1:η1)–(μ_2–η1:η1) and μ_3–(η1)–(μ_2–η1:η1) 1,4-ndc^{2-} ligands. (c) The green "single-bridge" is a μ_4–(μ_2–η1:η1)–(μ_2–η1:η1) 1,4-ndc^{2-} ligand. (d) The 3D framework of **2** with two kinds of channels (A and B) along the *b* axis, guest molecules [PMIm]$^+$ are removed for clarity (blue polymer = heptanuclear SBU).

ndc^{2-} ligands as linkers possess μ_3–(η1)–(μ_2–η1:η1) and μ_7–(μ_3–η2:η1)–(μ_4–η3:η1) coordination modes, for which the rare μ_7-coordinated 1,4-ndc^{2-} bridging mode is the first reported. Importantly, it distinguishes itself from the previous MOFs, because the heteronuclear SBU consists of the unprecedented windmill-like nonanuclear SBU [$Na_5Co_4Br(OCO)_{12}$]. Each SBU comprises a pentanuclear sodium cluster linked to four CoO_4 tetrahedra in a vertices-sharing fashion. A μ_5-Br^- links four Na(1) ions and one Na(2) to form a square pyramidal sodium cluster and the axial Na(2)–Br lies on the fourfold axis with the Na(2)···Na(1) separation of 3.31 Å. The two types of Na(1)···Na(1) distances are 3.84 Å and 5.44 Å. Such a sodium cluster connects to four Co(1) ions by the bridging interactions of μ_4–η3:η1, μ_3–η2:η1 and μ_2–η1:η1 carboxylates to afford a windmill-like heterometallic nonanuclear SBU $Na_5Co_4Br(COO)_{12}$, in which four Co(II) ions occupy the fan-shaped blade positions and share one plane with four Na(1) ions. The corresponding Co···Co separations are 7.42 Å and 10.50 Å. To date, heterometallic polynuclear SBUs containing transition metal ions and alkaline-earth metal ions have rarely been observed in MOFs.[15] Along the *c* axis orientation, the complicated [Co_4Na_5] SBUs further interact with each other forming an interesting 1D columnar structure through "four-fold-bridge" ligands in a μ_7-coordinate mode. Moreover, each 1D chain is connected to the surrounding four chains by four pairs of "double-bridge" ligands in a μ_3-bridging fashion, leading to a 3D 6-connected anionic framework (Fig. 3).

Systematic variation of the structures

Although a small but significant number of MOFs have been obtained in recent years under ionothermal conditions, systematically probing the effect of the length of a linear alkyl chain from the [C_nMIm]Br species is still lacking in the structural study of MOFs.

Changing the size of the IL cation does have some influence on the final structure – the larger sized IL forms the more open framework with the extra space needed to accommodate the large template (Fig. 4). Omitting the guest IL cations, the void volumes of the polymers were calculated to be 41.9% (**1**), 24.7% (**2**), 28.0% (**3**) and 36.2% (**4**) by PLATON. The trend of the void volume correlates with the size of the cations (except for polymer **1** with a 2D structure). The degree of the match between the cation size and host cavity decides the final construction. The effect of the ionic liquid on the composition of the MOFs was only studied by Kwon *et al.* in the system of Ni/Zn-H_3BTC (H_3BTC = 1,3,5-benzenetricarbonic acid)[6c,8] but the void volumes of MOFs obtained with various combinations of ionic liquids do not change regularly. The reason is probably that the length of the ligand BTC is not enough to hold long alkyl chains. Meanwhile, compared to dicarboxylic acids, BTC as a linker has various connection and coordination modes. More complex factors exist in the formation of the MOFs, which is not appropriate for exploring the influence of the size of ILs. Thus, an appropriate size of organic ligands is undoubtedly a key element in systematically discussing the influence of ILs on framework structures.

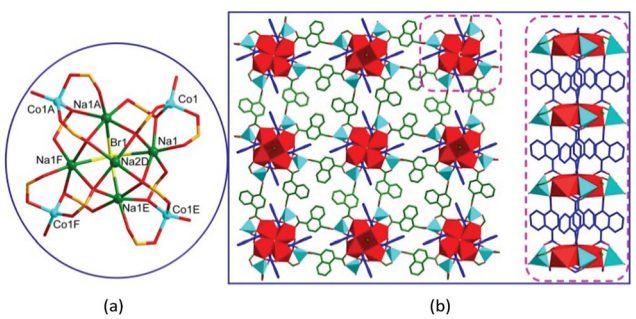

Fig. 3 (a) The nonanuclear heterometallic SBU structure of **4**. (b) View of the 3D anionic framework (left) and 1D chain unit (right) in **4**.

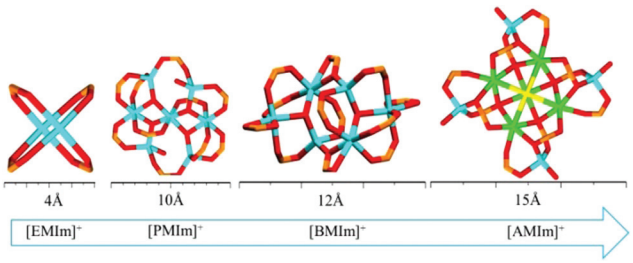

Fig. 4 Systematic vibration of SBUs with the different alkyl chains of the IL cations. The longer cations are inclined to form the larger SBUs (blue = Co center and green = Na center).

In addition, incorporating different imidazolium cations [C_nMIm]$^+$ (n = 2–5) as efficient structure-directing agents affects the structures of SBUs. The sizes of the SBUs of **1**–**4** are shown in Fig. 1, which demonstrates that the longer cations are inclined to form the larger SBUs and further achieve a stronger complementarity of spatial structure between the imidazolium cations. Although the construction of high nuclearity metal oxide clusters has been the goal of much research related to transition metal complexes,[16] an updated account on polynuclear transition metal clusters in ILs is still deficient,[17] especially lacking an effective method to construct large metal clusters rather than extended frameworks. We also tried several reaction ratios to explore whether the mole ratio can control the SBUs but only under the reported condition did we obtain the single crystals. Therefore, it is an amazing result and we will continue to study the link.

Thermogravimetric analysis

Thermogravimetric experiments were conducted to study the thermal stability of MOFs **1**–**4**, which is an important parameter of metal-organic frameworks. The TGA curves of **1**–**4** are shown in Fig. 5. For **1**, the complex does not undergo a significant mass loss below 300 °C, and then begins to decompose rapidly upon further heating. This confirms that there is no solvent molecule present in the structure, which conforms with the crystal structure. The remaining residue is presumed to be CoO (calcd, 16.14%; found, 18.66%). Similarly, **2** and **3**

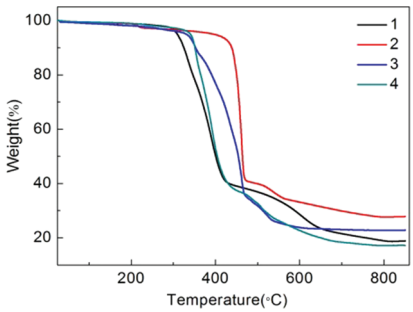

Fig. 5 TGA curves for polymers **1–4**.

respectively lose weight rapidly from 420 °C and 328 °C, and the final residual weights are 27.54% (calcd, 26.62%) for **2**, and 22.72% (calcd, 23.04%) for **3**, which correspond to the weight of CoO. The TGA curve of **4** indicates that the framework remains stable up to *ca.* 330 °C, the temperature at which the framework starts to decompose. The remaining residue may be a mixture of NaBr, Na_2O and CoO (calcd, 17.62%; found, 17.13%). The above thermal behavior may be attributed to their structural features. These results show the thermal stability of such complexes, although the decomposition temperatures of the ligands and cations of ILs are not distinguished for all the complexes.

Magnetic properties

The temperature dependence of the magnetic susceptibilities of **1–4** was measured between 2 and 300 K with an applied direct current (dc) magnetic field of 1000 Oe.

[Co(1,4-ndc)Br][EMIm] (1). The temperature dependence of $\chi_m T$ for **1** in the range of 2–300 K is shown in Fig. 6a. The $\chi_m T$ value of **1** at 300 K is 3.33 cm^3 K mol^{-1} (χ_m is the molar magnetic susceptibility per Co(II) ion), which is significantly larger than the spin-only value of 1.87 cm^3 K mol^{-1} for $S = 3/2$ and $g = 2$, indicating an orbital contribution for the high spin Co(II). The data of χ_m^{-1} in the range 49–300 K could be well fitted with the Curie–Weiss law to afford $C = 4.15$ cm^3 K mol^{-1} and $\theta = -73.19$ K. The negative θ value is indicative of the dominant antiferromagnetic (AF) interactions between two Co^{2+} ions *via* the Co–O–C–O–Co pathway. To investigate the dynamics of the magnetization, the alternative current (ac) magnetic susceptibility was studied as a function of both temperature and frequency. Both the in-phase (χ') and out-of-phase (χ'') components of the ac susceptibility exhibit obvious frequency-independent peaks at 4.9 K (Fig. S12†), confirming the presence of AF ordering.

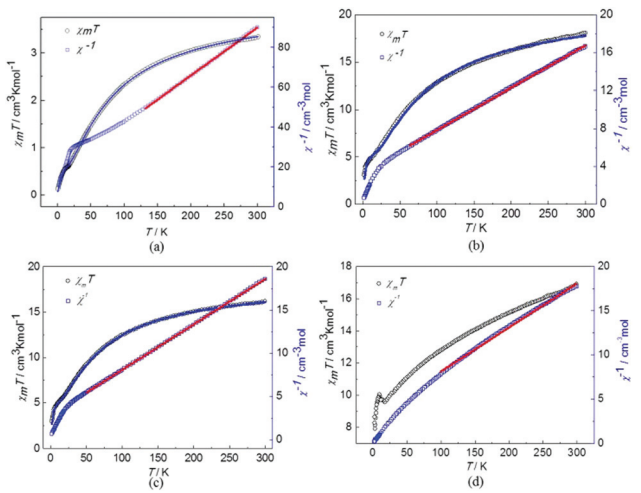

Fig. 6 The plots of the $\chi_m T$ and χ_m^{-1} *versus* T for **1–4** (a)–(d). The blue and red solid lines represent the best fit obtained from the exponential model described in the text and the Curie–Weiss law, respectively.

$[PMIm]_2[Co_7(1,4\text{-ndc})_6(OH)_4]$ (2). The value of $\chi_m T$ obviously decreases as the temperature decreases from 300 to 2 K (Fig. 6b). At room temperature (300 K), the $\chi_m T$ value is 18.05 cm^3 K mol^{-1} and substantially exceeds the value of 13.09 cm^3 K mol^{-1} expected for seven uncoupled Co(II) ions with $S = 3/2$ and $g = 2.0$. In the temperature region above 64 K, a typical paramagnetic Curie–Weiss behavior was observed with the Curie and Weiss constants being $C = 22.41$ cm^3 K mol^{-1} and $\theta = -75.48$ K, respectively. Both the negative θ value and the decrease of $\chi_m T$ are indicative of AF interactions between the neighbor Co(II) ions bridged by the carboxylate groups and μ_3-OH bridges, although strong spin–orbit coupling may contribute to the negative value as well.

$[BMIm]_2[Co_6(1,4\text{-ndc})_6(OH)_2]$ (3). As shown in Fig. 6c, the $\chi_m T$ value of 16.17 cm^3 K mol^{-1} at 300 K is much higher than the spin-only value of 11.25 cm^3 K mol^{-1} for six isolated high-spin Co^{2+} ions, which is a consequence of the orbital contribution. The data above 50 K obey the Curie–Weiss law with $C = 18.99$ cm^3 K mol^{-1} and $\theta = -52.93$ K, which clearly suggests a dominant AF coupling between the Co(II) ions. The existence of tightly interconnected Co(II) ions within the $[Co_6^{II}]$ hexameric SBUs implies that its magnetic groups at high temperature will be dominated by magnetic interactions within the SBUs. Unfortunately, the explanation of the magnetic behavior of $[Co_6^{II}]$ complexes is always difficult and exact calculations for deriving the J parameter from experimental data over the whole temperature range is impossible, due to the orbitally degenerate ground state of the six-coordinated ions.

$[AMIm]_4[Co_4Na_5(1,4\text{-ndc})_8Br]$ (4). The room temperature $\chi_m T$ value of 16.91 cm^3 K mol^{-1} per Co_4 unit is much higher than the spin-only value of 7.5 cm^3 K mol^{-1} for four free Co(II) ions ($S = 3/2$ and $g = 2.0$), which is common for the strong spin–orbit coupling of Co(II) ions (Fig. 6d). As the temperature decreases, the value of $\chi_m T$ reduces to 9.57 cm^3 K mol^{-1} at about 18 K, after which it rises abruptly to a sharp maximum (10.01 cm^3 K mol^{-1}) at 10 K, and finally drops again to 8.28 cm^3 K mol^{-1} at 2 K. The steep increase of the $\chi_m T$ value below 18 K is indicative of spontaneous magnetization originating possibly from a weak ferromagnetic exchange interaction caused by spin-canting, and the final decrease in $\chi_m T$ below 9 K indicates a magnetic phase transition. The data above 100 K obeys the Curie–Weiss law very well, giving a

Curie constant of C = 20.11 cm^3 K mol^{-1} and Weiss constant of θ = −63.55 K.

To further investigate the phase transformation at low temperature, the field-cooled (FC) and zero-field-cooled (ZFC) magnetization measurements were performed at a low applied field of 30 Oe at 2–30 K (Fig. S13†). At very low temperatures, the FC/ZFC curves undergo a slight increase which could be due to the presence of a paramagnetic contribution arising from defects in the crystal structure.[18] The ZFC and FC curves show a bifurcation below 10 K, suggesting the irreversible transition of the weak ferromagnetism. The magnetic behavior of **4** is further confirmed by the field-dependence of the magnetization measurement at 1.8 K. The isotherm magnetizations experience a rapid rise in M *vs.* H at the beginning of the low field, and then smoothly increase to the saturation magnetization of about 11.60$N\beta$ per Co_4 unit at 50 k Oe (Fig. S14†). The critical field H_c = 853 Oe is approximately detected by the sharp peak of the dM/dH *vs.* H curve, which confirms that the M *vs.* H curve increases rapidly at low fields, corroborating the presence of weak ferromagnetism due to spin-canting.[19] In addition, a small hysteresis loop was observed at 1.8 K with a remnant magnetization (M_r) of 0.02$N\beta$ and the canting angle α, related to M_r and saturated magnetization (M_s (unit $N\beta$) = gS) by sinα = M_r/M_s was estimated to be 0.095° (Fig. S15†).[20] No peaks were observed for both in-phase (χ') and out-of-phase (χ'') components of the ac susceptibility of **4** (Fig. S16†).

Conclusions

The successful systematic synthetic strategy presents four cobalt-MOFs with a size-change of the SBUs using an ionothermal method. Structural analyses indicate that matching the sizes of the cations with the cavities of frameworks favors the complicated 3D structures, while the smaller cation prefers the ordinary 2D layer. Further, tuning the size and shape of high nuclear Co-clusters plays a vital role in affecting the magnetic properties. The intrinsic value of this design approach lies in the ability to direct regular changes of secondary building blocks into extended networks in which specific properties can be targeted.

Acknowledgements

This work was supported by the National Natural Science Foundation of China, Innovation Scientists and Technicians Troop Construction Projects of Henan Province and the Natural Science Foundation of Henan Province of China.

References

1 (*a*) M. O. Yaghi, M. O'Keeffe, W. N. Ockwig, H. K. Chae, M. Eddaoudi and J. Kim, *Nature*, 2003, **423**, 705–714; (*b*) T. R. Cook, Y. R. Zheng and P. J. Stang, *Chem. Rev.*, 2013, **113**, 734–777; (*c*) D.-B. Dang, B. An, Y. Bai, G.-S. Zheng and J.-Y. Niu, *Chem. Commun.*, 2013, **49**, 2243–2245.

2 M. Eddaoudi, J. Kim, N. Rosi, D. Vodak, J. Wachter, M. O'Keeffe and O. M. Yaghi, *Science*, 2002, **295**, 469–472.

3 (*a*) D. J. Tranchemontagne, J. L. Mendoza-Cortes, M. O'Keeffe and O. M. Yaghi, *Chem. Soc. Rev.*, 2009, **38**, 1257–1283; (*b*) D. Moon and M. S. Lah, *Inorg. Chem.*, 2005, **44**, 1934–1940.

4 (*a*) D. Freudenmann, S. Wolf, M. Wolff and C. Feldmann, *Angew. Chem., Int. Ed.*, 2011, **50**, 11050–11060; (*b*) A. Thirumurugan and C. N. R. Rao, *Cryst. Growth Des.*, 2008, **8**, 1640–1644; (*c*) X. Sun and J. L. Anthony, *J. Phys. Chem. C*, 2012, **116**, 3274–3280.

5 D. N. Dybtsev, H. Chun and K. Kim, *Chem. Commun.*, 2004, 1594–1595.

6 (*a*) E. R. Parnham and R. E. Morris, *Acc. Chem. Res.*, 2007, **40**, 1005–1013; (*b*) J. Zhang, S. Chen and X. Bu, *Angew. Chem., Int. Ed.*, 2008, **47**, 5434–5437; (*c*) L. Xu, S. Yan, E. Y. Choi, J. Y. Lee and Y. U. Kwon, *Chem. Commun.*, 2009, 3431–3433; (*d*) Q. Y. Liu, W. L. Xiong, C. M. Liu, Y. L. Wang, J. J. Wei, Z. J. Xiahou and L. H. Xiong, *Inorg. Chem.*, 2013, **52**, 6773–6775; (*e*) R. E. Morris, *Chem. Commun.*, 2009, 2990–2998.

7 Z. Lin, D. S. Wragg, P. Lightfoot and R. E. Morris, *Dalton Trans.*, 2009, 5287–5289.

8 L. Xu, E.-Y. Choi and Y.-U. Kwon, *Inorg. Chem.*, 2007, **46**, 10670–10680.

9 B. An, Y. Bai, J. L. Wang and D. B. Dang, *Dalton Trans.*, 2014, **43**, 12828–12831.

10 E. R. Parnham and R. E. Morris, *Chem. Mater.*, 2006, **18**, 4882–4887.

11 (*a*) G. M. Sheldrick, *SHELXS-97, Programs for X-ray Crystal Structure Solution*, University of Göttingen, Göttingen, Germany, 1997; (*b*) G. M. Sheldrick, *SHELXL-97, Programs for X-ray Crystal Structure Refinement*, University of Göttingen, Göttingen, Germany, 1997.

12 B. Tan, Z.-L. Xie, X.-Y. Huang and X.-R. Xiao, *Inorg. Chem. Commun.*, 2011, **14**, 1001–1003.

13 (*a*) A. Ferguson, A. Parkin, J. Sanchez-Benitez, K. Kamenev, W. Wernsdorfer and M. Murrie, *Chem. Commun.*, 2007, 3473–3475; (*b*) K. G. Alley, R. Bircher, O. Waldmann, S. T. Ochsenbein, H. U. Gu1del, B. Moubaraki, K. S. Murray, F. Fernandez-Alonso, B. F. Abrahams and C. Boskovic, *Inorg. Chem.*, 2006, **45**, 8950–8957; (*c*) L. F. Chibotaru, L. Ungur, C. Aronica, H. Elmoll, G. Pilet and D. Luneau, *J. Am. Chem. Soc.*, 2008, **130**, 12445–12455.

14 (*a*) K. S. Gavrilenko, S. V. Punin, O. Cador, S. p. Golhen, L. n. Ouahab and V. V. Pavlishchuk, *J. Am. Chem. Soc.*, 2005, **127**, 12246–12253; (*b*) X.-Y. Wang and S. C. Sevov, *Inorg. Chem.*, 2008, **47**, 1037–1043; (*c*) H. Kumagai, Y. Oka, S. Kawata, M. Ohba, K. Inoue, M. Kurmoo and H. Ōkawa, *Polyhedron*, 2003, **22**, 1917–1920.

15 (*a*) G. E. Kostakis, A. M. Ako and A. K. Powell, *Chem. Soc. Rev.*, 2010, **39**, 2238–2271; (*b*) L. Kayser, R. Pattacini, G. Rogez and P. Braunstein, *Chem. Commun.*, 2010, **46**, 6461–6463; (*c*) S. Xiang, X. Wu, J. Zhang, R. Fu, S. Hu and X. Zhang, *J. Am. Chem. Soc.*, 2005, **127**, 16352–16353.

16 (*a*) S. H. Zhang, N. Li, C. M. Ge, C. Feng and L. F. Ma, *Dalton Trans.*, 2011, **40**, 3000–3007; (*b*) Y. F. Bi, X. T. Wang, W. P. Liao, X. F. Wang, X. W. Wang, H. J. Zhang and S. Gao, *J. Am. Chem. Soc.*, 2009, **131**, 11650–11651; (*c*) S. D. Han, W. C. Song, J. P. Zhao, Q. Yang, S. J. Liu, Y. Li and X. H. Bu, *Chem. Commun.*, 2013, **49**, 871–873; (*d*) Y. Peng, C. B. Tian, H. B. Zhang, Z. H. Li, P. Lin and S. W. Du, *Dalton Trans.*, 2012, **41**, 4740–4743.

17 (*a*) E. Ahmed and M. Ruck, *Dalton Trans.*, 2011, **40**, 9347–9357; (*b*) H.-S. Liu, Y.-Q. Lan and S.-L. Li, *Cryst. Growth Des.*, 2010, **10**, 5221–5226; (*c*) J.-W. Ji, W. Zhang, G.-X. Zhang and Z.-B. Han, *Inorg. Chem. Commun.*, 2009, **12**, 956–958.

18 F.-P. Huang, J.-L. Tian, D.-D. Li, G.-J. Chen, W. Gu, S.-P. Yan, X. Liu, D.-Z. Liao and P. Cheng, *CrystEngComm*, 2010, **12**, 395.

19 P.-K. Chen, Y.-X. Che, J.-M. Zheng and S. R. Batten, *Chem. Mater.*, 2007, **19**, 2162–2167.

20 K. L. Hu, M. Kurmoo, Z. Wang and S. Gao, *Chem. – Eur. J.*, 2009, **15**, 12050–12064.